

Original Article

Angiopietin-1 gene-modified human mesenchymal stem cells promote angiogenesis and reduce acute pancreatitis in rats

Jie Hua*, Zhi-Gang He*, Dao-Hai Qian, Sheng-Ping Lin, Jian Gong, Hong-Bo Meng, Ting-Song Yang, Wei Sun, Bin Xu, Bo Zhou, Zhen-Shun Song

*Department of Hepatobiliary and Pancreatic Surgery, Shanghai Tenth People's Hospital, Tongji University School of Medicine, Shanghai, China. *Equal contributors.*

Received May 23, 2014; Accepted July 1, 2014; Epub June 15, 2014; Published July 1, 2014

Abstract: Mesenchymal stem cells (MSCs) can serve as a vehicle for gene therapy. Angiopietin-1 (ANGPT1) plays an important role in the regulation of endothelial cell survival, vascular stabilization, and angiogenesis. We hypothesized that ANGPT1 gene-modified MSCs might be a potential therapeutic approach for severe acute pancreatitis (SAP) in rats. Human umbilical cord-derived MSCs with or without transfection with lentiviral vectors containing the ANGPT1 gene were delivered through the tail vein of rats 12 h after induction of SAP. Administration of MSCs alone significantly reduced pancreatic injury and inflammation, as reflected by reductions in pancreatitis severity scores and serum amylase and lipase levels as well as reducing the serum levels of proinflammatory cytokines (TNF- α , IFN- γ , IL-1 β , and IL-6). Furthermore, administration of ANGPT1-transfected MSCs resulted in not only further reductions in pancreatic injury and serum levels of proinflammatory cytokines, but also promotion of pancreatic angiogenesis. These results suggest that MSCs and ANGPT1 have a synergistic role in the treatment of SAP. ANGPT1 gene-modified MSCs may be developed as a potential novel therapy strategy for the treatment of SAP.

Keywords: Angiopietin-1, mesenchymal stem cells, acute pancreatitis, gene therapy

Introduction

Acute pancreatitis (AP), a common necroinflammatory condition of the pancreas, remains an unsolved clinical problem. In 80% of patients, AP is mild and self-limiting, but in up to 20%, AP is complicated by substantial morbidity and mortality [1]. Despite efforts to start an appropriate treatment, mortality rate of severe attacks has not substantially decreased during the past two decades [2]. It is now generally accepted that AP is initiated by premature activation of proenzymes within acinar cells, thereby leading to autodigestion of the pancreatic gland [3]. Local inflammation is then initiated with production of inflammatory cytokines such as interleukin (IL)-1, IL-6, tumor necrosis factor- α (TNF- α), and interferon- γ (IFN- γ) [4, 5]. Additionally, chemokines such as monocyte chemoattractant protein-1 (MCP-1) and fractalkine (FKN), are demonstrated to play an important role in promoting distant organ failure (i.e.,

pulmonary failure) [6-8]. Furthermore, microcirculatory derangements like leukocyte-endothelial cell interaction and perfusion failure result in enhancement of microvascular permeability to these inflammatory mediators, playing a pivotal role in the progression of the acutely altered pancreatic tissue [1]. The releasing of both inflammatory cytokines and chemokines make the disease develop, with the occurrence of systemic inflammatory response syndrome, multiple organ failure, or even death [9]. However, despite decades of research, few therapeutic strategies for severe acute pancreatitis (SAP) have emerged, and current specific options for treatment are still limited [10].

Mesenchymal stem cells (MSCs), since first described by Friedenstein et al [11], have been used for the treatment of a number of diseases that currently have limited or no treatment options [12]. In the past ten years, numerous studies have shown MSCs can improve tissue

repair and reduce inflammation via producing a number of cytokines [13-15] or homing to injured tissues or sites of inflammation [16-18]. In addition, MSCs may also promote angiogenesis in ischemic tissues by expressing hypoxia inducible factor-1 α (HIF- α) [19]. Therefore, MSCs may have beneficial effects in their own right in the treatment of SAP.

Angiopoietin 1 (ANGPT1) plays an essential role in embryonic vascular development as a ligand for the receptor-tyrosine kinase Tie2. In the postnatal state, ANGPT1 is responsible for a quiescent vascular phenotype and is known as an endothelial survival and vascular stabilization factor that reduces endothelial permeability and inhibits leukocyte-endothelium interactions by modifying endothelial cells adhesion molecules and cell junctions [20, 21]. Several studies have demonstrated its anti-inflammatory [22], anti-permeability [21], angiogenic [23], and endothelial protective characteristics [24]. Based upon this, we hypothesized that ANGPT1 gene transfer may be beneficial in the therapy of SAP.

The combination of MSCs and ANGPT1 gene therapy has proven successful in the treatment of myocardial infarction [25], acute lung injury [16], cerebral ischemia [26], and ischemic limb disease [23]. This dual strategy not only allows cells to engraft in the injured tissues, but also provides therapeutic proteins and other cellular products of interest. Therefore, the aim of this study was to evaluate the effect of MSCs alone or in combination with ANGPT1 on pancreatic injury, inflammation, and angiogenesis in a rat model of SAP.

Materials and methods

Isolation, culture, and characterization of MSCs

Umbilical cord matrix (UCM)-derived MSCs were used for this study because of their high accessibility, painless acquisition, and high proliferative capacity. Umbilical cords were taken from healthy women with pregnancies during elective cesarean section after obtaining informed consent (approved by the Tongji University Institutional Review Board). To perform cell isolation, the cords were cut into approximately 5-cm long segments, which were subsequently cut longitudinally to expose the

umbilical vein. Blood vessels (two arteries and one vein) were removed from each segment and the Wharton's jelly was carefully separated from the amniotic membrane. Then the cords were cut into 1-cm pieces and some incisions were made on the inner matrix. The pieces were transferred to 6-well plates (Corning Costar, NY, USA), one piece in each well, and covered completely with the culture medium that consisted of Dulbecco's Modified Eagle's Medium-Low Glucose (DMEM-LG; Invitrogen, Grand Island, NY, USA), 10% lot-selected fetal bovine serum (FBS; Biological Industries, Kibbutz Beit Haemek, Israel), 100 units/ml penicillin (Invitrogen), 100 μ g/ml streptomycin (Invitrogen), and 2 mM L-glutamine (Invitrogen). The medium was replaced every 2 days and the cord pieces were left in the medium for two weeks to ensure enough MSCs migrate from the Wharton's jelly to the wells. Then the remnants of the cord pieces were removed from the wells and cells attached to the wells were cultured until they were 80% confluent. The cells were detached with 0.25% trypsin and 1 mM ethylenediaminetetraacetic acid for 1 minute, resuspended with the culture medium, and seeded at a density of 1.0×10^4 cells/cm² in 100-mm dishes (Corning) for expansion. Passage 2 UCM-MSCs were characterized by expression of cell surface markers with flow cytometry and trilineage differentiation capacities or frozen with protein-free cryopreservation medium (Cyagen Biosciences, CA, USA) at 1.0×10^6 cells/ml in liquid nitrogen for further use.

For flow cytometry analysis, UCM-MSCs were labeled with the selected antibodies CD105-PerCP-Cy5.5, CD31-PE, CD45-PE, CD73-APC, CD34-PE, CD11b-PE, CD90-FITC, CD44-PE, CD19-PE, CD146-PE, and HLA-DR-PE and corresponding isotype controls (BD Biosciences, San Jose, CA, USA), and analyzed using a BD FACSCanto™ II flow cytometry system (BD Biosciences). Differentiation of UCM-MSCs was evaluated using a Human Mesenchymal Stem Cell Differentiation Kit (Cyagen Biosciences). Osteogenic and adipogenic differentiation assays were performed in 6-well tissue culture plates, and chondrogenic differentiation assay was performed using a pellet culture system in 15-ml polypropylene culture tubes. All assays were conducted according to the manufacturer's instructions.

MSCs-ANGPT1 treatment of SAP in rats

Production of lentiviral vectors and transfection of UCM-MSCs

The ANGPT1 open reading frame was cloned from a human cDNA library and was amplified by polymerase chain reaction (PCR) using the primers: 5'-GAGGATCCCCGGGTACCGGTCGCCA CCATGACAGTTTTCTTCTTCTTTG-3' (Forward) and 5'-TCACCATGGTGGCGACCGGAAAATCTAAA GGTCGAATCATC-3' (Reverse). The ANGPT1 cDNA were inserted into the AgeI site of the pUbi-MCS-EGFP expression lentiviral vector (pGV208) to generate pGV-ANGPT1. Lentiviral vector without therapeutic gene was used as control (pGV-EGFP). Then the vectors were individually transfected into 293T cells using Lipofectamine 2000 (Invitrogen) for propagation. The cells were transfected with respective vector for 5 h and a subsequent recovery period of 36 h in DMEM supplemented with 10% FBS. Fluorescence microscopy and western blotting were performed to determine transfection efficiency and expression efficiency of ANGPT1.

Before being used, the above lentiviral vectors, expressing either enhanced green fluorescence protein (EGFP) only or both EGFP and ANGPT1, were evaluated for their viral titer. The viral titers of Lenti-ANGPT1 and Lenti-EGFP were 1×10^8 and 1×10^9 TU/ml, respectively.

To select the best multiplicity of infection (MOI) for lentivirus-mediated gene transfer, UCM-MSCs were exposed to lentiviral vectors at MOI of 1, 10, and 100 for 12 h. Fluorescence microscopy was used to observe transfection efficiency and cell viability according to EGFP expression and cell morphology. The optimal MOI was chosen for both highest EGFP expression and viability.

Detection of ANGPT1 expression in MSCs after transfection

ANGPT1 expression of UCM-MSCs was detected by RT-PCR, Western blot, and ELISA. Total RNA was extracted from UCM-MSCs 72 h after transfection with TRIzol reagent (Invitrogen). For cDNA synthesis, 2 μ g of RNA were reverse transcribed using 500 ng of oligo (dT) primers and the SuperScript II First Strand Synthesis System (Invitrogen) according to the manufacturer's indications. The ANGPT1 PCR primer

sequences were: forward 5'-GGGGGAGGTTG GACTGTAAT-3' and reverse 5'-AGGGCACATTTG CACATACA-3' (362 bp); the human glyceraldehyde-3-phosphate dehydrogenase (GAPDH) primer sequences were: forward 5'-ACCACA GTCCATGCCATCAC-3' and reverse 5'-TCCACCAC CCTGTTGCTGTA-3' (452 bp). The PCR was initiated at 95°C for 1min, followed by denaturation at 95°C for 15 s, annealing at 58°C for 15 s, and extension at 72°C for 45 s for 40 cycles. The PCR products were subject to electrophoresis on 2% agarose gels.

For Western blot, cells were washed twice with cold PBS and lysed in extraction buffer (50 mM Tris-HCl pH7.4, 150 mM NaCl, 1 mM PMSF, 1 mM EDTA, 1% Triton X-100, and 0.1% SDS). The whole cell lysate samples were centrifuged at 10,000 g at 4°C for 15 min. Protein concentration was measured using the Bradford method, and protein lysates were aliquoted and stored at -70°C until used. The proteins (40 μ g/lane) were separated by 10% SDS-polyacrylamide gel electrophoresis and electroblotted onto PVDF membrane by standard procedures. The membrane was blocked with 5% non-fat milk in Tris-buffered saline containing 0.1% Tween-20 (TBST) overnight at 4°C. On the second day, the membrane was incubated with goat polyclonal anti-ANGPT1 antibody (1:1000 dilution, Santa Cruz Biotechnology, CA, USA) for 2 h, followed by horseradish peroxidase conjugated anti-goat secondary antibody (1:1000 dilution, Santa Cruz Biotechnology) for 1 h at room temperature. Then the membrane was washed in TBST and developed using an enhanced chemiluminescence (ECL) detection system (Santa Cruz Biotechnology).

ANGPT1-specific ELISA was performed using the Quantikine Human Angiopoietin-1 Immunoassay (R&D Systems, Minneapolis, Minnesota, USA). The supernatant samples were collected from UCM-MSCs cultures in 6-well plates at 2-day intervals for up to 15 days after transfection.

Animal model of severe acute pancreatitis and cell transplantation protocol

Male Sprague-Dawley rats weighing 180-220 g were used for the experiment. The present study conforms to the Guide for the Care and Use of Laboratory Animals published by the US

MSCs-ANGPT1 treatment of SAP in rats

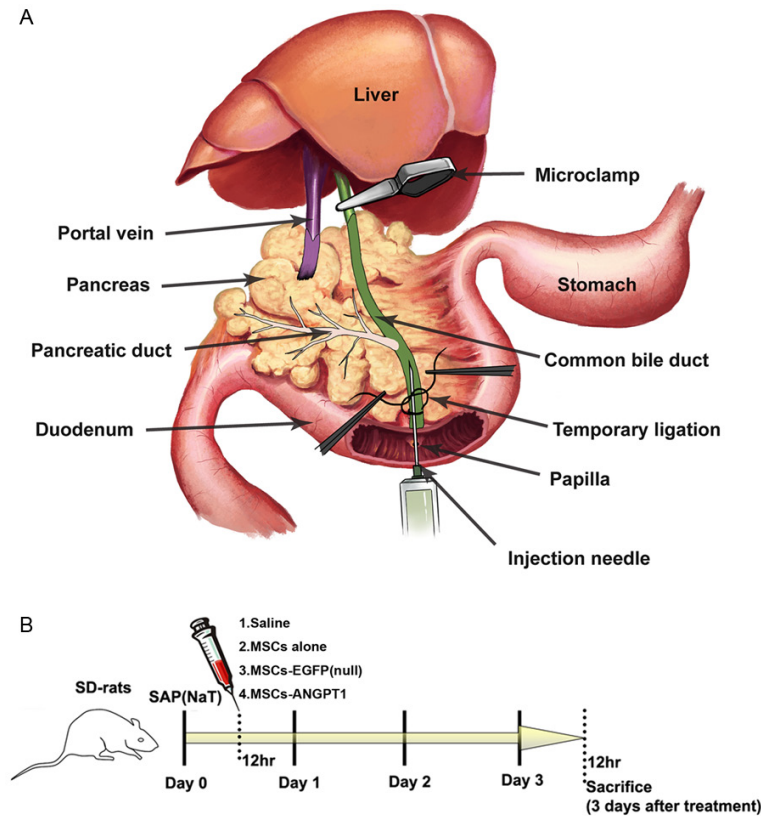


Figure 1. Animal model of acute pancreatitis and experimental scheme for in vivo study. A: After puncture of the common bile duct using a 24-G blunt-tipped needle, a temporary ligation was performed in the distal part of the common bile duct to prevent leakage of sodium taurocholate solution. Injection of the solution into the liver was prevented by placing a microclamp at the proximal common bile duct. Sodium taurocholate solution was then retrogradely infused into pancreatic duct over a 60-second period. B: SD-rats initially received sodium taurocholate by retrograde pancreatic duct infusion, followed by intravenous injection 12 hours later with saline, MSCs, MSCs-EGFP, or MSCs-ANGPT1. Rats were then sacrificed 3 days after to evaluate the cell migration and therapeutic effects. NaT, sodium taurocholate; SAP, severe acute pancreatitis; SD-rats, Sprague-Dawley rats.

National Institutes of Health (NIH Publication No.85-23, revised 1996) and animal procedures were approved by the Institutional Animal Care and Use Committee of Tongji University (Shanghai, China).

The animals were anesthetized by intraperitoneal injection of pentobarbital (50 mg/kg body weight). A 2-cm midline laparotomy was performed and the first loop of duodenum was identified. The duodenum was flipped over to expose the pancreas and was immobilized with a 6-0 traction suture, and the papilla of Vater was identified. A puncture was made on the wall of the duodenum directly opposite to the papilla with a 20-G needle and a 24-G blunt-tipped needle catheter was passed through the

puncture wound, and then into the common bile duct via the papilla of Vater. The tip of the needle catheter was placed 5 mm into the bile duct, well before the entry of the pancreatic duct. Then the catheter was secured in that position with a 8-0 prolene ligature and the proximal common bile duct was occluded at the liver hilum with a microclamp (**Figure 1A**). A NaCl solution (1 ml/kg) of 3% sodium taurocholate (Sigma-Aldrich, St Louis, Missouri, USA) was retrogradely injected into the bile-pancreatic duct over a 60-second period. Then the needle catheter, the microclamp, as well as the securing ligature were removed. The puncture site was closed using a 6-0 prolene suture, and the abdomen was closed in two layers with 4-0 prolene sutures. Subcutaneous buprenorphine hydrochloride injection was given immediately after wound closure. The animals were given free access to water and normal laboratory chow 6 hours after the operation.

Saline, MSCs, MSCs transfected with pGV-EGFP (MSCs-EGFP, null-transfected MSCs), and MSCs transfected with pGV-ANGPT1 (MSCs-ANGPT1) (2.0×10^6 cells in 200 μ l saline for each rat) were slowly infused via the tail vein 12 hours after the operation (**Figure 1B**). Chloromethylbenzamido-1,1'-dioctadecyl-3,3',3'-Tetramethylindocarbocyanine Perchlorate (CM-Dil) was used to label cells before injection into the animals. CM-Dil was selected as the tracking system as it does not affect cell division or cell differentiation and was stable for six weeks during long-term cell transplantation studies [27]. Briefly, cells were incubated with 2 μ M CM-Dil for 5 minutes at 37°C and for additional 15 minutes at 4°C, and were visualized for fluorescent staining under fluorescence microscopy (Leica, DMI6000B, Germany).

MSCs-ANGPT1 treatment of SAP in rats

Sacrifice was performed 3 days after UCM-MSCs treatment, and blood samples were obtained and centrifuged (400 g, 30 minutes, 4°C). Serum samples were then collected and stored at -70°C until assaying. The pancreas was dissected, rinsed in cold PBS and halved. One half was fixed overnight in 10% neutral buffered formaldehyde and embedded in paraffin. The other half was protected from light and fixed in 4% paraformaldehyde-PBS at 4°C for 4 h, then rinsed three times in cold PBS and transferred in PBS-30% sucrose at 4°C overnight for cryopreservation. Tissues were then embedded in Tissue Tek OCT compound and snap-frozen.

Histopathology

Paraffin sections of 5 µm were cut and stained with hematoxylin and eosin (H&E). Tissue sections were evaluated using light microscopy at 10× magnification. For each animal, three independent sections were evaluated by two separate observers in a blinded manner. Grading of pancreatitis severity was performed using a scale from 0 to 4 for the degree of edema (0 = absent; 1 = diffuse expansion of interlobar septa; 2 = diffuse expansion of interlobular septa; 3 = diffuse expansion of interacinar septa; 4 = diffuse expansion of intercellular septa), inflammation (0 = absent; 1 = around ductal margin; 2 = in parenchyma, < 50% of lobules; 3 = in parenchyma, 50%-75% of lobules; 4 = in parenchyma, >75% of lobules), vacuolization (0 = absent; 1 = periductal, < 5%; 2 = focal, 5%-20%; 3 = diffuse, 21%-50%; 4 = severe, >50%), and necrosis (0 = absent; 1 = 1-4 necrotic cells/high-power field [HPF]; 2 = 5-10 necrotic cells/HPF; 3 = 11-15 necrotic cells/HPF; 4 ≥ 16 necrotic cells/HPF).

Measurement of amylase, lipase, myeloperoxidase, cytokines, and chemokines

Serum amylase activity was measured by a colorimetric assay kit (BioVision, Milpitas, CA, USA) using ethylidene-pNP-G7 as the substrate. The chromophore in 50 µl serum was measured spectrophotometrically at 405 nm. The absorbance was linear to the enzyme activity. Serum lipase levels were also measured by a colorimetric assay kit (BioVision) according to the manufacturer's instructions. The method is based on the principle that lipase hydrolyzes a

triglyceride substrate to form glycerol, which is quantified enzymatically via monitoring a linked change in the OxiRed probe absorbance at 570 nm. The concentrations of amylase and lipase were expressed as units per liter (U/L).

Neutrophil infiltration within the pancreas was detected by measuring tissue myeloperoxidase (MPO) activity as previously described. Briefly, pancreas specimens were homogenized in 50 mM phosphate buffer (pH 6.0) containing 0.5% hexadecyltrimethylammonium bromide. The suspensions were subjected to three cycles of freezing and thawing and further disrupted by sonication (40 seconds). Then the samples were centrifuged (10,000 g, 5 min, 4°C), and supernatants were used for the MPO assay. The supernatant (50 µl) was incubated in reaction solution consisting of 1.6 mM tetramethylbenzidine, 80 mM sodium phosphate buffer, and 0.3 mM hydrogen peroxidase at 37°C for 2 min, and absorbance at 655 nm was recorded. The results were corrected in terms of protein concentration, and MPO activity was expressed as units per milligram of protein (U/mg).

Serum cytokines (TNF-α, IFN-γ, IL-1β, IL-4, IL-6, and IL-10) and chemokines (MCP-1 and FKN) were measured with rat-specific Quantikine ELISA Kits (R&D Systems) according to the manufacturer's instructions.

Immunohistochemistry and evaluation of vascular density

Immunohistochemistry was performed on sections (5 µm) from formalin-fixed pancreatic tissues. The sections were dewaxed, rehydrated, and incubated in hydrogen peroxide solution for 5 minutes to block endogenous peroxidases. Then, mouse monoclonal anti-CD31 antibody (IgG1 clone P2B1, Abcam, Cambridge, UK) was applied to the sections at a 1:100 dilution for 1 hour at room temperature, followed by biotinylated rabbit anti-mouse secondary antibody and streptavidin-horseradish peroxidase conjugate for 30 minutes. The sections were developed with 3-amino-9-ethylcarbazole (AEC) substrate (Boster Biotechnology, Wuhan, China) for 5 minutes, and then counterstained with hematoxylin and mounted.

To determine the microvascular density (MVD), sections of pancreatic tissues that stained with CD31 antibody were used. According to previous recommendations [28], all independent

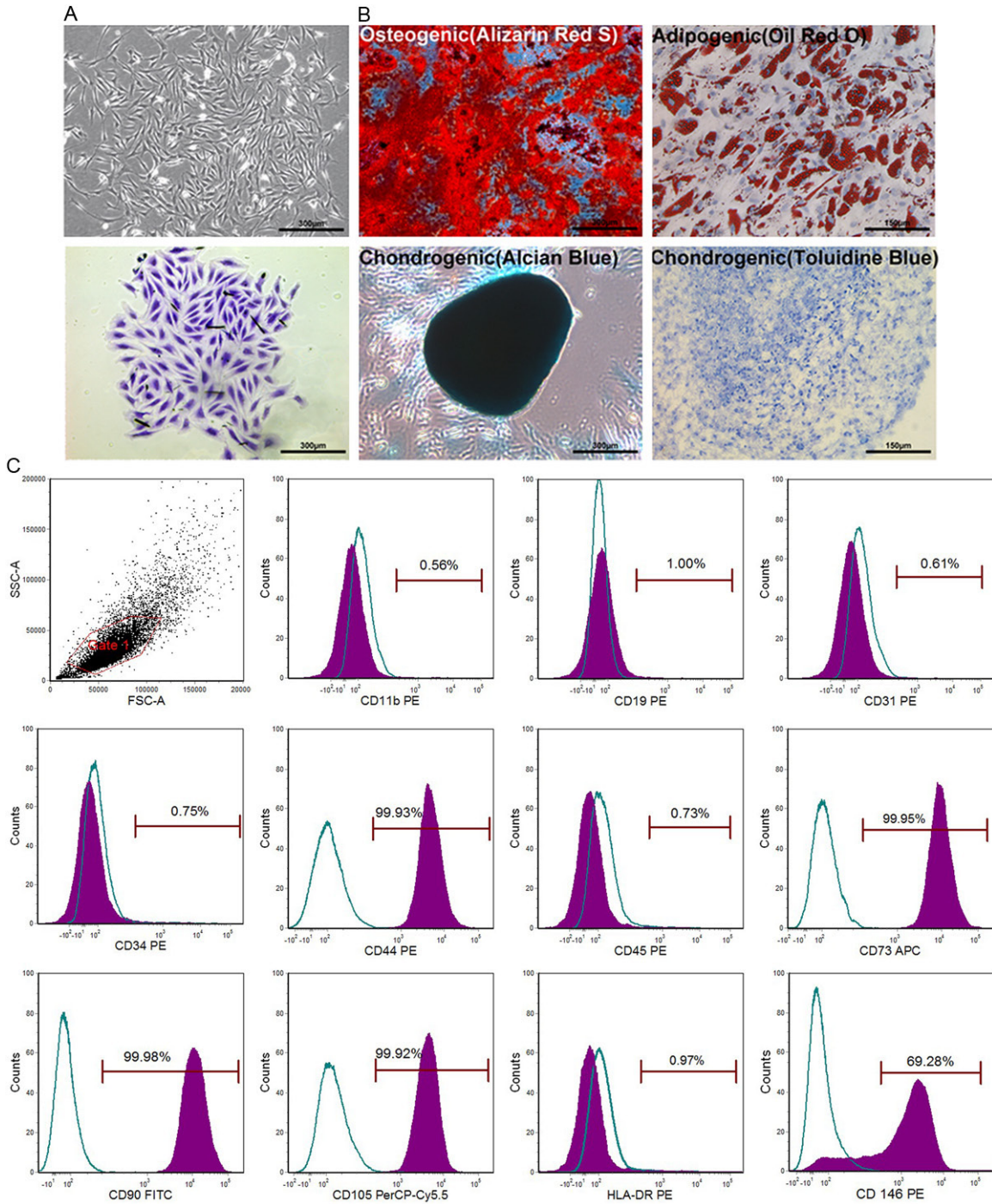


Figure 2. Characterization of MSCs isolated from human umbilical cord matrix. A: Fibroblast-like UCM-MSCs and crystal violet staining of a single cell-derived colony of UCM-MSCs for clear visualization. B: Multilineage differentiation capacity of UCM-MSCs: osteogenic, adipogenic, and chondrogenic differentiation. C: Surface marker expression of UCM-MSCs by flow cytometry.

CD31-positive structures were counted, irrespective of the presence of an identifiable lumen. MVD was calculated by dividing the total number of microvessels by the area of each

section (expressed as vessels/mm²). Values reported for each experimental condition correspond to the average values were obtained from 8 individual animals.

MSCs-ANGPT1 treatment of SAP in rats

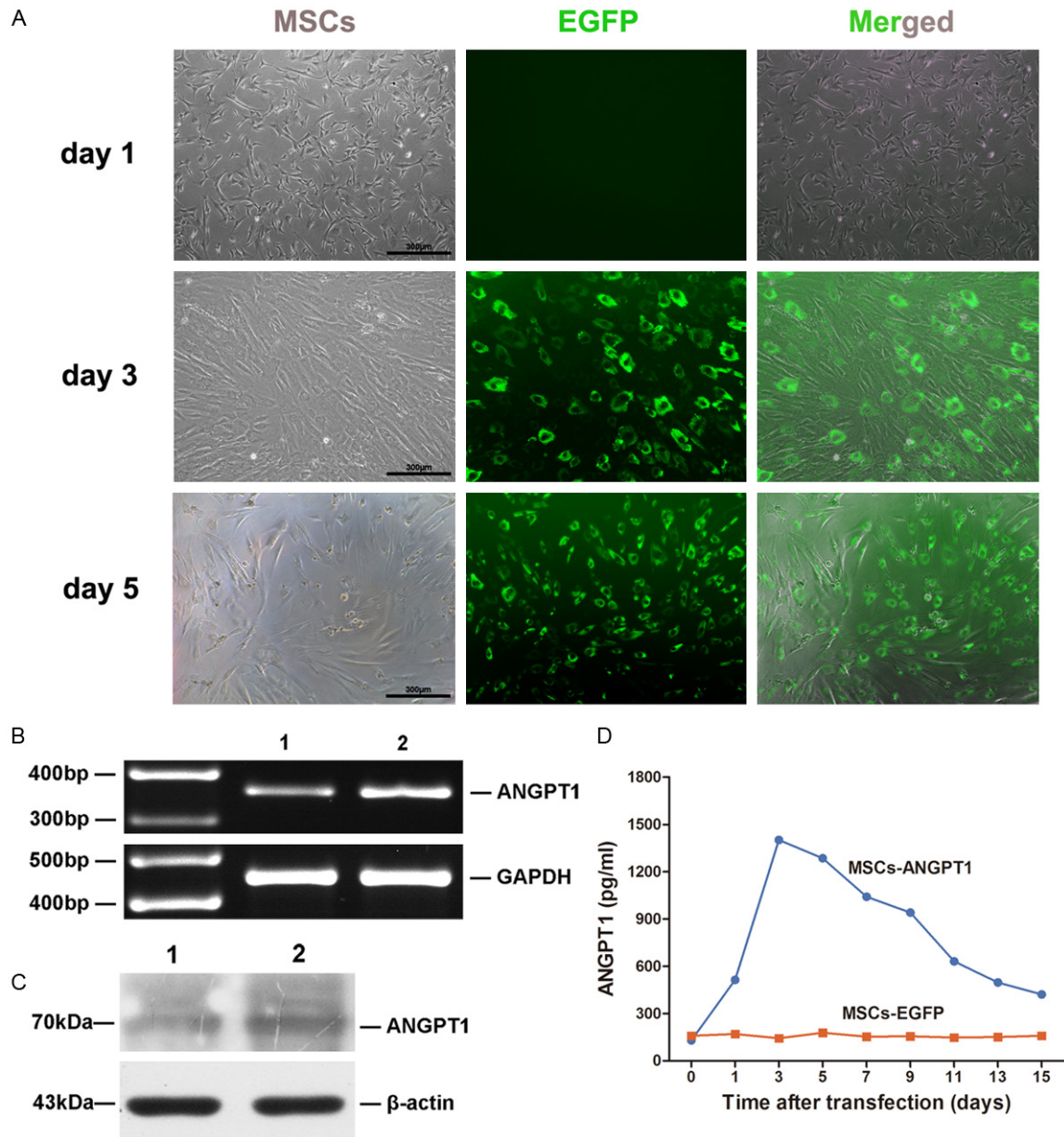


Figure 3. Detection of ANGPT1 expression in MSCs after transfection. **A:** The expression of EGFP was detectable on day 3 after transfection at a MOI of 100 with high cell viability and transfection efficiency (>95%). **B:** RT-PCR detection of ANGPT1 in MSCs 3 days post-transfection. The ANGPT1 mRNA in ANGPT1-transfected MSCs (lane 2) was more evident than in EGFP-transfected MSCs (lane 1). **C:** Western blot detection of ANGPT1 expression 3 days post-transfection. The expression of ANGPT1 protein in ANGPT1-transfected MSCs (lane 2) was higher than in EGFP-transfected MSCs (lane 1). **D:** Detection of ANGPT1 secretion in cell culture supernatants at different time points by ELISA. The level of ANGPT1 in ANGPT1-transfected MSCs culture medium reached 1400 pg/ml on day 3 and remained at a high level over a 1-week period, while in EGFP-transfected MSCs culture medium, the level of ANGPT1 maintained at a low level of less than 300 pg/ml.

Statistical analysis

Data were presented as means \pm standard deviations (SD). Comparisons between two groups were made with the use of unpaired two-tailed Student's *t* tests using SPSS software (SPSS 12.0, Chicago, IL). *P* < 0.05 was considered statistically significant.

Results

Characterization and ANGPT1 transfection of MSCs

The isolated cells showed fibroblast-like shapes when cultured on plastic culture plates (**Figure 2A**). The cells were demonstrated to differenti-

MSCs-ANGPT1 treatment of SAP in rats

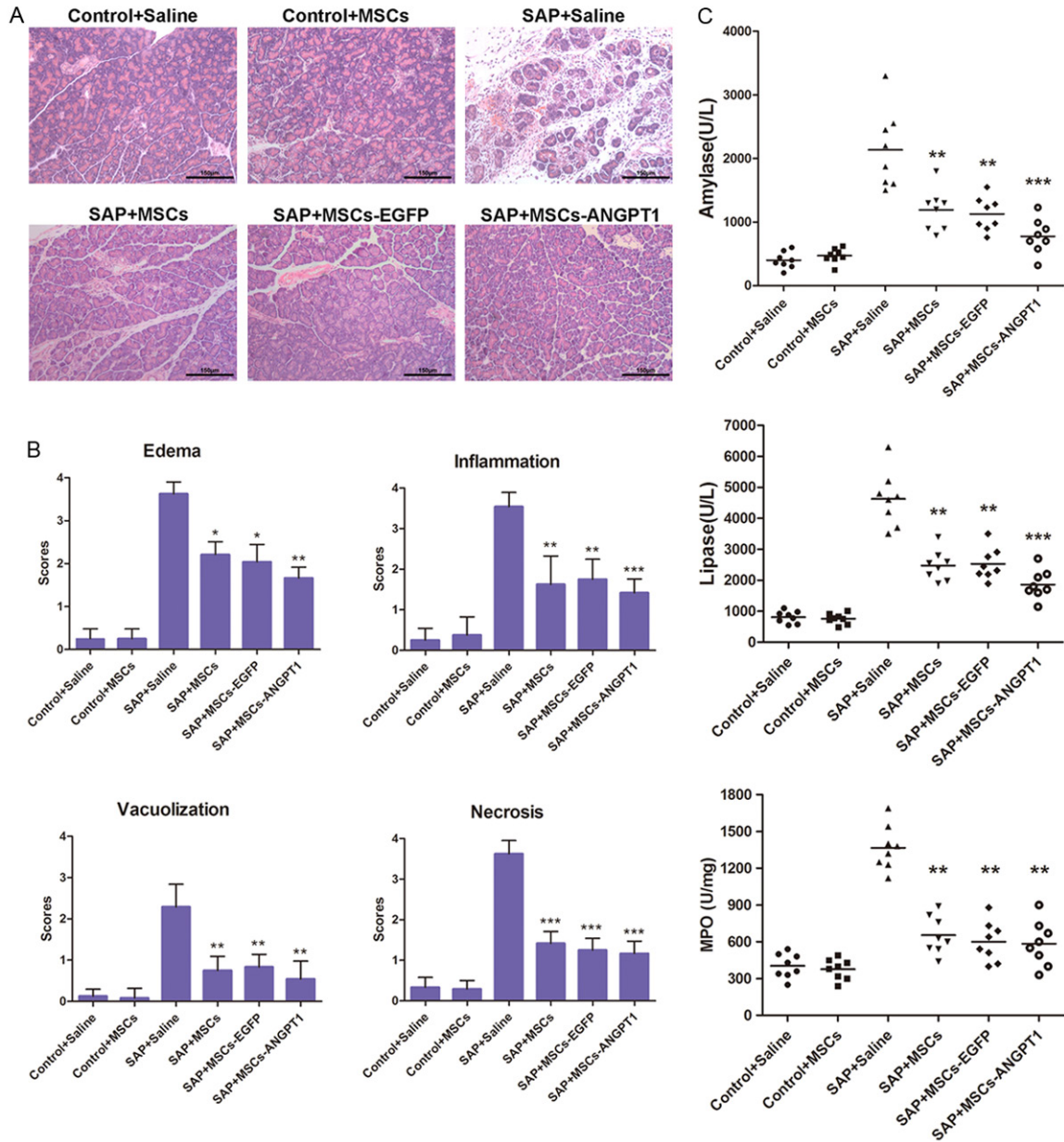


Figure 4. Effects of MSCs and MSCs-ANGPT1 on pancreatic histopathology and markers. A: Representative images of hematoxylin and eosin stained pancreatic sections from 6 experimental groups. B: Histological analysis of pancreatitis severity. Each value represents the mean \pm standard deviation of scores from eight randomly chosen microscopic fields of eight independent sections. C: Activities of amylase (U/L), lipase (U/L), and MPO (U/mg). * $P < 0.05$, ** $P < 0.01$, and *** $P < 0.001$, compared between the SAP+saline group and each treated group (MSCs, MSCs+EGFP, or MSCs+ANGPT1). N = 8 per group.

ate into three predominant mesenchymal lineages: osteocytes, adipocytes, and chondrocytes (Figure 2B). The cells were uniformly positive for CD44, CD73, CD90, and CD105 by flow cytometry, and were negative for CD11b (monocyte marker), CD19 (B-cell marker), CD31 (endothelial cell marker), CD34 (endothelial cell marker), CD45 (leukocyte marker), or HLA-DR.

In addition, nearly 70% of these cells were positive for CD146, which is a marker of multipotency (Figure 2C).

To determine the transfection efficiency, MSCs were infected with lentiviral vectors (pGV-ANGPT1 or pGV-EGFP) at MOI of 1, 10, and 100 for 12 h. We found that MSCs tolerated an MOI of

100 well and the expression of EGFP was detectable on day 3 after transfection with high cell viability and transfection efficiency (>95%) assessed by fluorescence microscopy (**Figure 3A**). To further determine the expression of ANGPT1 by ANGPT1-modified MSCs, RT-PCR, Western blot, and ELISA were performed. A specific band corresponding to an expected 362bp PCR product was observed and it was more evident in ANGPT1-transfected MSCs than in EGFP-transfected MSCs (**Figure 3B**). Western blot also showed a 70 kDa-specific band in ANGPT1-transfected MSCs, indicating an obviously increased expression of ANGPT1 protein (**Figure 3C**). The ELISA results also revealed a markedly higher levels of ANGPT1 in ANGPT1-transfected MSCs culture medium compared with EGFP-transfected MSCs culture medium (**Figure 3D**).

Effect of MSCs and MSCs-ANGPT1 on pancreatic histopathology and markers

Histological assessment of pancreatic sections 3 days after induction of SAP revealed evidence of marked edema, inflammation, vacuolization, and necrosis, which was significantly reduced in animals receiving MSCs, MSCs-EGFP, or MSCs-ANGPT1 (**Figure 4A**). Severity of pancreatic injury was scored using a histopathology score system, which evaluates the pancreatic injury in four categories: edema, inflammation, vacuolization, and necrosis. Although treatment with MSCs, MSCs-EGFP, or MSCs-ANGPT1 reduced pancreatitis severity, the differences among these three groups did not reach statistical significance (**Figure 4B**).

Serum amylase activity was significantly elevated 3 days after saline infusion in SAP rats (**Figure 4C**). MSCs alone treatment markedly decreased serum amylase levels ($P < 0.01$), which was more apparent in rats treated with MSCs-ANGPT1 ($P < 0.001$). Similar results were observed in serum lipase activity with a reduction of about 50%. MPO is an enzyme that is found predominantly in the azurophilic granules of polymorphonuclear leukocytes (PMN). Tissue MPO activity is frequently utilized to estimate tissue PMN accumulation in inflamed tissues and correlates significantly with the number of PMN determined histochemically in tissues. As was expected, pancreatic MPO activity was markedly increased in SAP animals receiving saline infusion, which was suppressed sig-

nificantly in the treatment groups (MSCs, MSCs-EGFP, or MSCs-ANGPT1).

Effect of MSCs and MSCs-ANGPT1 on inflammatory cytokines and chemokines

To further evaluate the inflammation actions by MSCs and MSCs-ANGPT1, levels of inflammatory cytokines and chemokines were measured with serum samples collected from animals. As shown in **Figure 5**, proinflammatory cytokines (TNF- α , IFN- γ , IL-1 β , and IL-6) were all elevated in SAP+saline group compared with the two control groups. Treatment with MSCs and MSCs-ANGPT1 significantly reduced the levels of these proinflammatory cytokines. The levels of anti-inflammatory cytokines (IL-4 and IL-10) in SAP rats receiving saline infusion were lower than the control groups, whereas they were dramatically increased in SAP animals treated with MSCs and MSCs-ANGPT1. In addition, SAP also increased the serum level of MCP-1, an important chemokine in the pathogenesis of pancreatitis, whereas treatment with MSCs and MSCs-ANGPT1 attenuated this increase. Another chemokine FKN was also elevated 3 days after induction of SAP. Although MSCs and MSCs-ANGPT1 infusion in SAP rats tended to decrease the serum level of FKN, the results did not differ significantly from saline infusion.

Effect of MSCs and MSCs-ANGPT1 on pancreatic angiogenesis

To evaluate pancreatic angiogenesis after cell transplantation, immunohistochemical staining of pancreatic sections was performed by using the endothelial cell-specific antibody CD31. In normal control groups treated with saline or MSCs, capillary vessels were observed in the periacinar space with small and round shapes. The CD31-positive structures were scattered in the SAP+saline group, while in the treated groups (MSCs, MSCs-EGFP, or MSCs-ANGPT1) they were obvious. Numerous vascular structures with varying thickness were detectable in the SAP+MSCs-ANGPT1 group (**Figure 6A**). The MSCs-ANGPT1 group had a markedly higher vascular density than both MSCs-alone and MSCs-EGFP groups ($P < 0.05$, **Figure 6B**).

Detection of MSCs and MSCs-ANGPT1 in rat pancreas

CM-Dil-labeled cells retained the proliferative ability with fibroblast-like shapes in *in vitro* cul-

MSCs-ANGPT1 treatment of SAP in rats

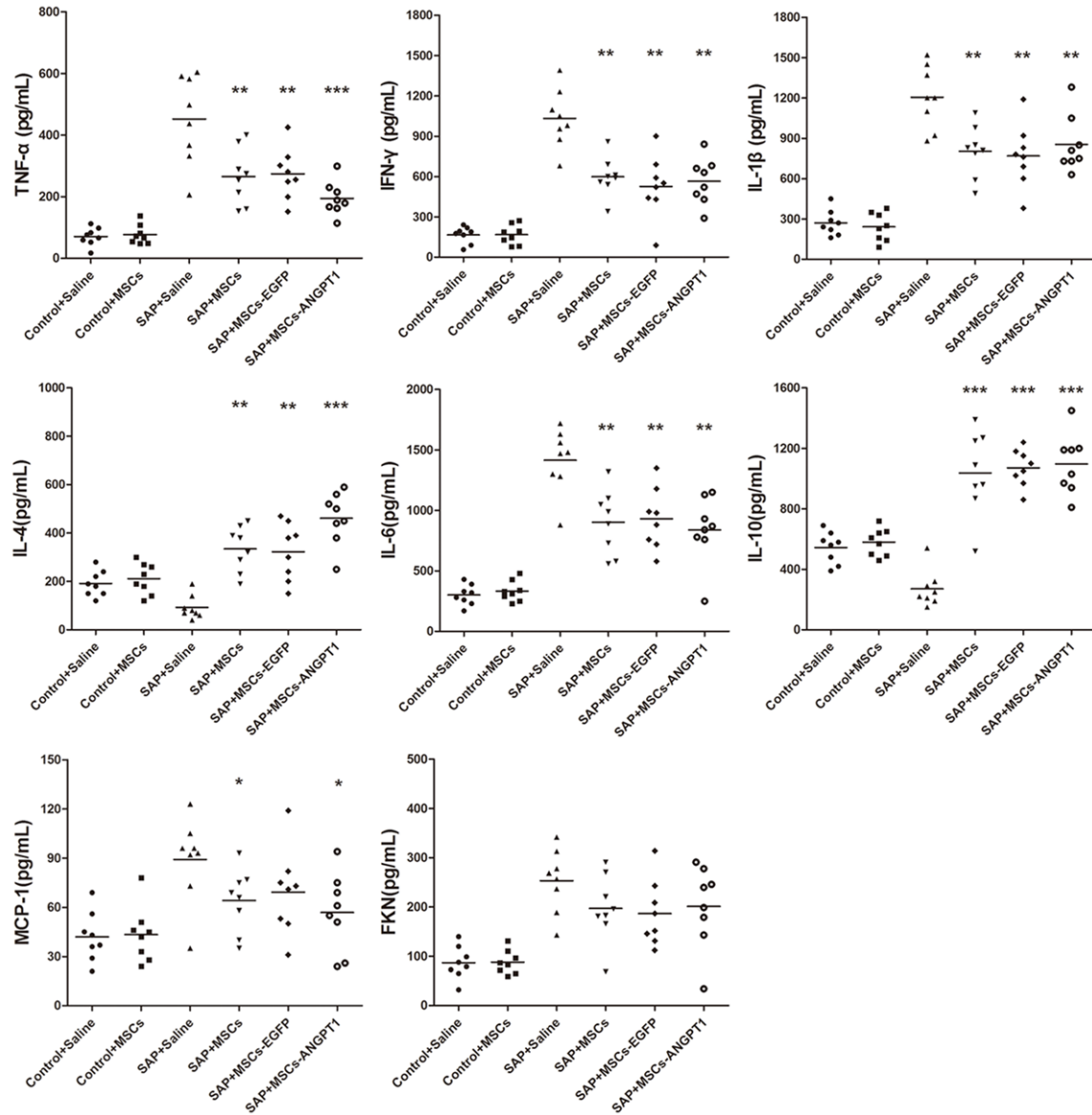


Figure 5. Effect of MSCs and MSCs-ANGPT1 on inflammatory cytokines and chemokines. Levels of inflammatory cytokines (TNF- α , IFN- γ , IL-1 β , IL-4, IL-6, and IL-10) and chemokines (MCP-1 and FKN) were measured using ELISA. * $P < 0.05$, ** $P < 0.01$, and *** $P < 0.001$, compared between the SAP+saline group and each treated group (MSCs, MSCs+EGFP, or MSCs+ANGPT1). $N = 8$ per group.

ture, indicating the stability of MSCs after labeling process (Figure 7A). MSCs migration to the injured pancreas was verified by confocal microscopy. MSCs labeled with fluorescent tracking dye CM-Dil were observed in pancreatic sections 3 days after infusion (Figure 7B). Interestingly, the MSCs-infused groups with pancreatic injury showed a higher number of labeled MSCs than the MSCs-infused group without pancreatic injury (Figure 7C). Cell migration of MSCs-ANGPT1 treated group was

comparable with that of non- or null-transfected MSCs treated groups. No cell-specific red fluorescence was observed in sections from animals that did not receive CM-Dil-labeled MSCs.

Discussion

In this study, we found that MSCs could be transfected with the recombinant lentivirus (pGV-ANGPT1) with high expression of ANGPT1 while maintaining high cell viability. We also

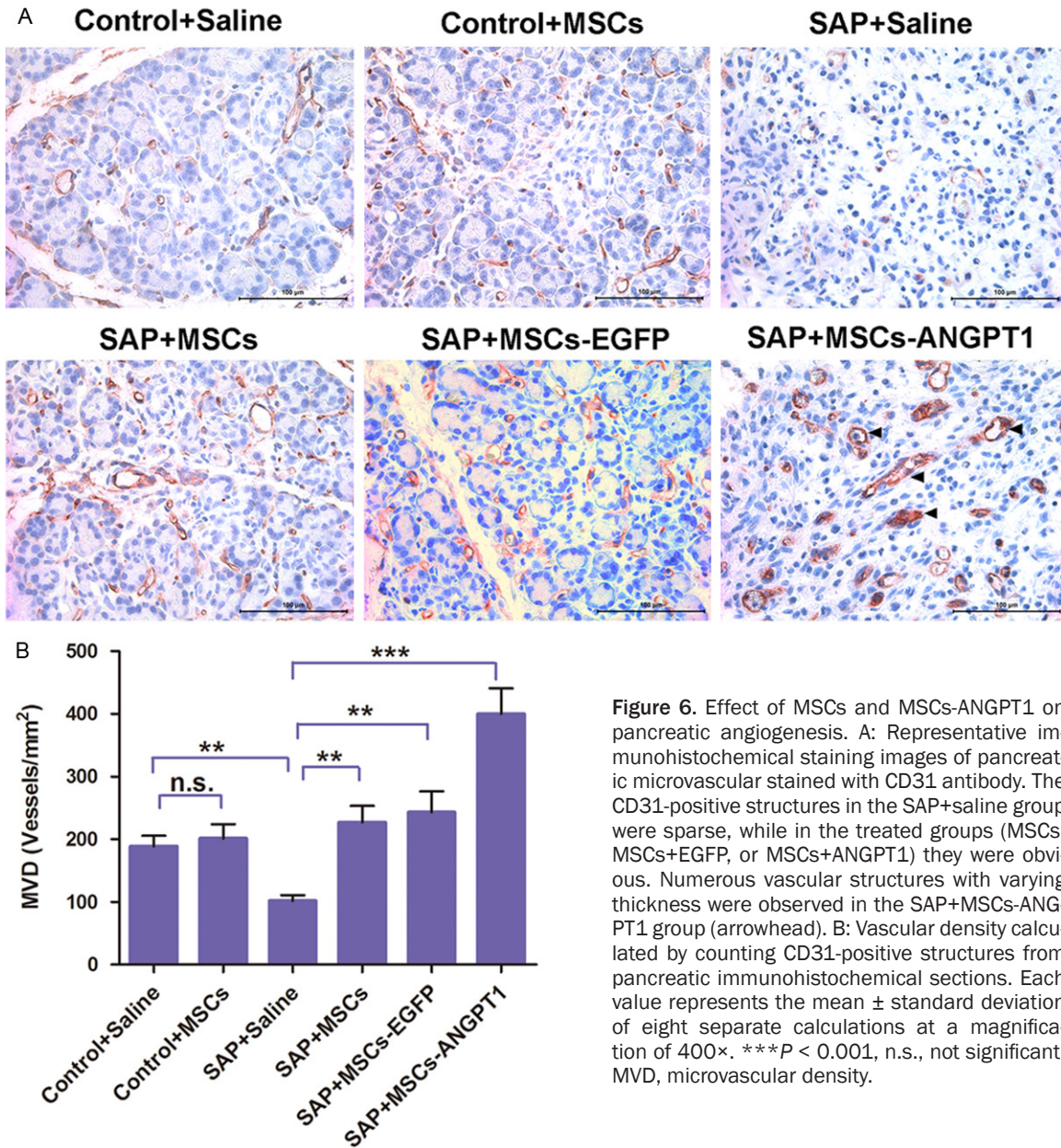


Figure 6. Effect of MSCs and MSCs-ANGPT1 on pancreatic angiogenesis. **A:** Representative immunohistochemical staining images of pancreatic microvasculature stained with CD31 antibody. The CD31-positive structures in the SAP+saline group were sparse, while in the treated groups (MSCs, MSCs+EGFP, or MSCs+ANGPT1) they were obvious. Numerous vascular structures with varying thickness were observed in the SAP+MSCs-ANGPT1 group (arrowhead). **B:** Vascular density calculated by counting CD31-positive structures from pancreatic immunohistochemical sections. Each value represents the mean \pm standard deviation of eight separate calculations at a magnification of 400 \times . *** $P < 0.001$, n.s., not significant. MVD, microvascular density.

demonstrated that MSCs exerted a beneficial therapeutic effect in the treatment of SAP by reducing inflammation, whereas administration of ANGPT1-transfected MSCs resulted in further improvement in both inflammation and angiogenesis. These findings suggested that ANGPT1-transfected MSCs could serve as a more effective therapy for SAP.

Cell-based gene therapy has been proved to be effective in the treatment of various diseases [29-31]. Since MSCs have the ability to efficiently home to sites of tissue injury and are immune privileged, the combination of MSCs

and gene therapy may provide additive benefits. Indeed, studies have investigated the therapeutic effects of MSCs-based gene therapy in many diseases, even in solid tumors, providing novel therapy strategies for these refractory diseases [16, 23, 25, 26, 32].

The choice of the most appropriate therapeutic gene is a critical determinant of the potential efficacy of a gene therapy strategy, and requires a detailed understanding of the pathogenic mechanisms underlying the target disorder [33]. SAP is an inflammatory disease which is initially caused by the unregulated activation of

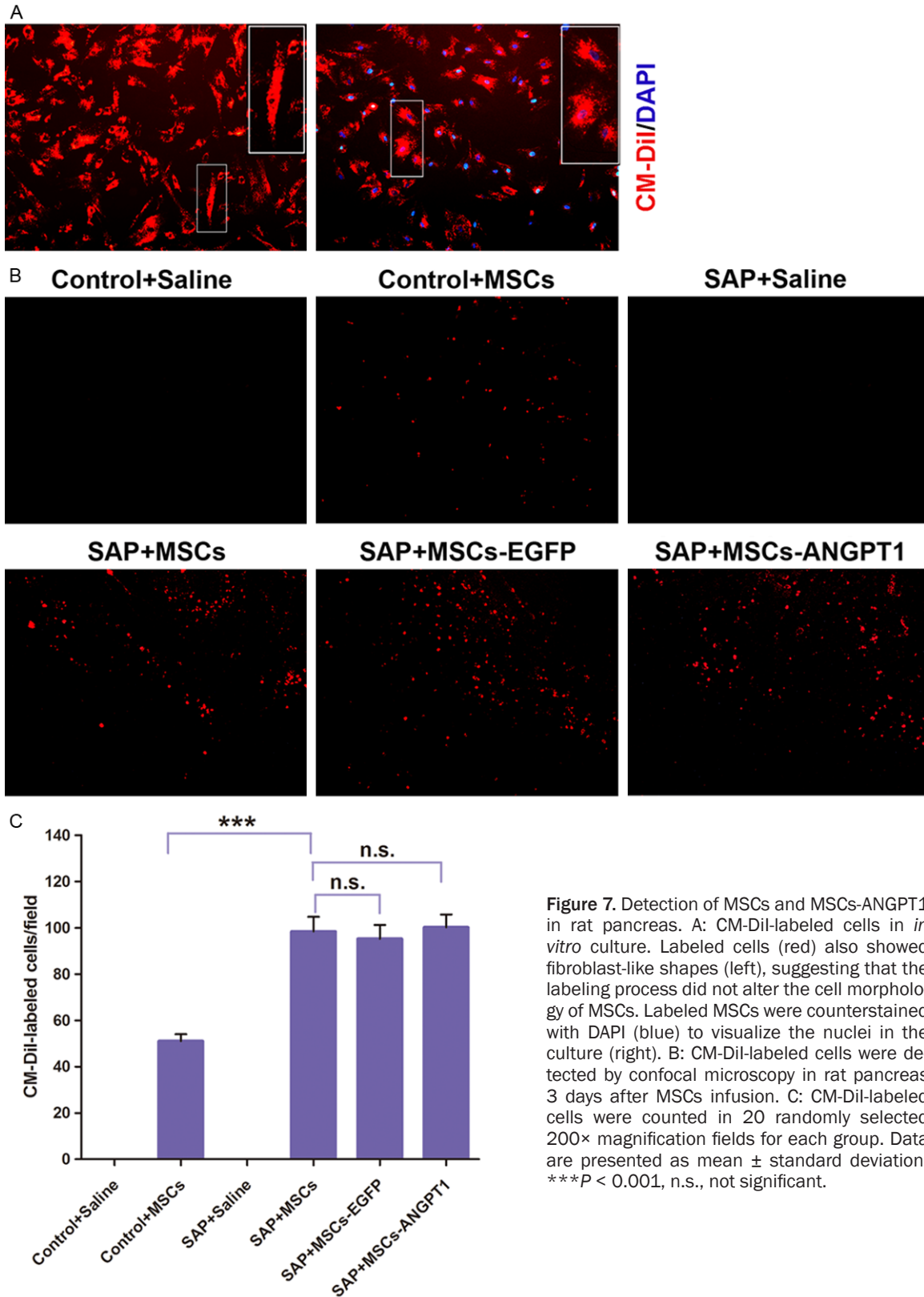


Figure 7. Detection of MSCs and MSCs-ANGPT1 in rat pancreas. **A:** CM-Dil-labeled cells in *in vitro* culture. Labeled cells (red) also showed fibroblast-like shapes (left), suggesting that the labeling process did not alter the cell morphology of MSCs. Labeled MSCs were counterstained with DAPI (blue) to visualize the nuclei in the culture (right). **B:** CM-Dil-labeled cells were detected by confocal microscopy in rat pancreas 3 days after MSCs infusion. **C:** CM-Dil-labeled cells were counted in 20 randomly selected 200× magnification fields for each group. Data are presented as mean ± standard deviation. *** $P < 0.001$, n.s., not significant.

trypsin within the pancreatic acinar cells. Then the production of inflammatory mediators and

chemokines contributes to the injury. In addition, activation of endothelial cells enables the

transendothelial migration of leukocytes, which release other harmful enzymes. Activation of endothelial cells is also accompanied by the enhancement of microvascular permeability in particular to large molecules, thereby leading to edema formation in the acutely inflamed pancreatic tissue [34]. ANGPT1, the natural agonist for Tie2, has been found to be associated with the activation of endothelial cells in response to inflammatory cytokines [33]. Given its anti-inflammatory, anti-permeability, angiogenic, and endothelial protective characteristics, we believe adding it to MSCs would improve pancreatic microcirculation, and therefore improve the therapeutic outcome of SAP.

The observed therapeutic effect of MSCs alone in SAP was not entirely unexpected, since MSCs can suppress T cells, dendritic cells, and natural killer cells, thereby reducing the secretion of pro-inflammatory cytokines (TNF- α , IFN- γ , IL-1 β , and IL-6), increasing the release of anti-inflammatory cytokines (IL-4, and IL-10), and inducing a tolerant phenotype [35, 36]. As MSCs have the ability to home to sites of inflammation and then enhance tissue repair, the observed MSCs engraftment in pancreas may explain the pathologic improvements in SAP. In addition, previous reports by our group [37] and others [38] have also demonstrated the therapeutic effect of MSCs for SAP, adding the evidence for the use of MSCs in SAP.

In the present study, there was an additional effect of ANGPT1-transfected MSCs compared with MSCs alone, not only on inflammatory cytokines and pancreatic histopathology, but also on pancreatic angiogenesis. This may be due to ANGPT1 protein produced by engrafted MSCs. As it directly targets to endothelial cell-to-cell junctions and has a major role in maintaining the integrity of endothelial monolayers [21], thus reducing capillary leakage with fluid loss into the pancreatic interstitium and leukocyte transmigration. Therefore, the observed further reduction in edema and inflammation in the SAP+MSCs-ANGPT1 group may be attributed to ANGPT1-induced inhibition of permeability. ANGPT1 has been found to be angiogenic both in development and in vitro and was used to promote angiogenesis for ischemic diseases, such as myocardial infarction [25]. In our study, SAP rats receiving ANGPT1-transfected MSCs resulted in a significant increased MVD, nearly twice than the control groups, confirming

the strong angiogenic effect of ANGPT1. Interestingly, near complete normalization of vascular density was achieved with MSCs alone delivery. A recent study by Edwards SS et al [39] revealed that UCM-MSCs have a strong expression of several well-characterized growth factors, such as VEGF-A, ANGPT1, and aFGF, which are directly linked to angiogenesis. They have also demonstrated in vitro and in vivo angiogenic capacity of UCM-MSCs through tubule formation and chicken chorioallantoic membrane assay. Thus, the increased vascular density observed in the SAP+MSCs group in our study may be attributed to the natural angiogenic effect of UCM-MSCs.

On a separate note, we were unable to detect a significant decrease in serum FKN level after injection of ANGPT1-transfected MSCs or MSCs alone. We believe that this is due to the early elevation of serum level of FKN in SAP. In a recent study in which the role of FKN was evaluated in the development of SAP, the authors found that serum FKN level reached a peak at 16 h after the induction of SAP and then declined in the subsequent time [40]. In our study, we detected serum FKN level 3 days after MSCs or saline treatment, which was much later than 16 hours. The time-dependent serum FKN level makes it not elevated as high as expected in the SAP+Saline group and therefore not significantly different between MSCs treatment and saline treatment groups. However, there is still a downward trend in serum FKN level after MSCs or MSCs-ANGPT1 treatment.

It is important to recognize certain limitations of this study. First of all, as SAP is usually accompanied by systemic complications, such as multiple organ failure, whether MSCs-ANGPT1 will be beneficial to other organs under this disease condition is unknown. Therefore, it will be necessary to explore the therapeutic capacity of MSCs-ANGPT1 in other related models, such as pancreatitis-associated lung injury and renal injury. As well, more than 20% of patients may suffer from impaired pancreatic functions (both endocrine and exocrine functions) after SAP [41], so it is important to determine whether this therapy strategy helps to improve pancreatic functions following pancreatitis, especially β -cell function. A further limitation relates to the use of lentiviral vectors, which may bring potential biological hazards

although it is so-called “suicide” lentivirus. The translation of the promising results of this study into an effective new therapy of SAP in patients will require, at the very least, that these limitations be addressed.

In conclusion, we have shown that UCM-MSCs significantly inhibited inflammation, decreased pancreatic injury, and promoted pancreatic angiogenesis in SAP models. However, this effect was greatly potentiated when these cells were engineered to overexpress the vasculo-protective factor ANGPT1. Our data show, to our knowledge for the first time, the synergistic action of combined cell and gene therapy for SAP, and may provide a basis for the development of an innovative approach for the treatment of SAP.

Acknowledgements

We thank Fei Yin (Central Laboratory, Shanghai Tenth People’s Hospital) for technical assistance. We also thank Feng Xing (Department of Obstetrics and Gynecology, Shanghai Tenth People’s Hospital) for providing umbilical cords. This work was partially supported by grants from the National Natural Science Foundation of China [No.81170436] and the Science and Technology Commission of Shanghai Municipality [No.114119a4500].

Disclosure of conflict of interest

None.

Address correspondence to: Dr. Zhenshun Song, Department of Hepatobiliary and Pancreatic Surgery, Shanghai Tenth People’s Hospital, Tongji University School of Medicine, 301 Yanchang Road, Shanghai 200072, China. Tel: +86 137 6120 5962; Fax: +86 021 6630 7365; E-mail: zs_song@hotmail.com

References

[1] Lund H, Tønnesen H, Tønnesen MH and Olsen O. Long-term recurrence and death rates after acute pancreatitis. *Scand J Gastroenterol* 2006; 41: 234-238.

[2] McKay CJ and Imrie CW. The continuing challenge of early mortality in acute pancreatitis. *Br J Surg* 2004; 91: 1243-1244.

[3] Chan YC and Leung PS. Acute pancreatitis: animal models and recent advances in basic research. *Pancreas* 2007; 34: 1-14.

[4] Bhatia M, Wong FL, Cao Y, Lau HY, Huang J, Puneet P and Chevali L. Pathophysiology of acute pancreatitis. *Pancreatology* 2005; 5: 132-144.

[5] Frossard JL, Steer ML and Pastor CM. Acute pancreatitis. *Lancet* 2008; 371: 143-152.

[6] Ishibashi T, Zhao H, Kawabe K, Oono T, Egashira K, Suzuki K, Nawata H, Takayanagi R and Ito T. Blocking of monocyte chemoattractant protein-1 (MCP-1) activity attenuates the severity of acute pancreatitis in rats. *J Gastroenterol* 2008; 43: 79-85.

[7] Huang L, Ma J, Tang Y, Chen P, Zhang S, Zhang Y and Yuan YZ. siRNA-based targeting of fractalkine overexpression suppresses inflammation development in a severe acute pancreatitis rat model. *Int J Mol Med* 2012; 30: 514-520.

[8] Huang LY, Chen P, Xu LX, Zhou YF, Zhang YP and Yuan YZ. Fractalkine upregulates inflammation through CX3CR1 and the Jak-Stat pathway in severe acute pancreatitis rat model. *Inflammation* 2012; 35: 1023-1030.

[9] Bhatia M, Brady M, Shokuhi S, Christmas S, Neoptolemos JP and Slavin J. Inflammatory mediators in acute pancreatitis. *J Pathol* 2000; 190: 117-125.

[10] Bhatia M. Novel therapeutic targets for acute pancreatitis and associated multiple organ dysfunction syndrome. *Curr Drug Targets Inflamm Allergy* 2002; 1: 343-351.

[11] Friedenstein AJ, Piatetzky-Shapiro II and Petrakova KV. Osteogenesis in transplants of bone marrow cells. *J Embryol Exp Morphol* 1966; 16: 381-390.

[12] Caplan AI and Correa D. The MSC: an injury drugstore. *Cell Stem Cell* 2011; 9: 11-15.

[13] Lee RH, Pulin AA, Seo MJ, Kota DJ, Ylostalo J, Larson BL, Semprun-Prieto L, Delafontaine P and Prockop DJ. Intravenous hMSCs improve myocardial infarction in mice because cells embolized in lung are activated to secrete the anti-inflammatory protein TSG-6. *Cell Stem Cell* 2009; 5: 54-63.

[14] Ortiz LA, Dutreil M, Fattman C, Pandey AC, Torres G, Go K and Phinney DG. Interleukin1receptor antagonist mediates the antiinflammatory and antifibrotic effect of mesenchymal stem cells during lung injury. *Proc Natl Acad Sci U S A* 2007; 104: 11002-11007.

[15] Sato K, Ozaki K, Oh I, Meguro A, Hatanaka K, Nagai T, Muroi K and Ozawa K. Nitric oxide plays a critical role in suppression of T-cell proliferation by mesenchymal stem cells. *Blood* 2007; 109: 228-234.

[16] Xu J, Qu J, Cao L, Sai Y, Chen C, He L and Yu L. Mesenchymal stem cell-based angiotensin-1 gene therapy for acute lung injury induced by lipopolysaccharide in mice. *J Pathol* 2008; 214: 472-481.

MSCs-ANGPT1 treatment of SAP in rats

- [17] Cheng Z, Ou L, Zhou X, Li F, Jia X, Zhang Y, Liu X, Li Y, Ward CA, Melo LG and Kong D. Targeted migration of mesenchymal stem cells modified with CXCR4 gene to infarcted myocardium improves cardiac performance. *Mol Ther* 2008; 16: 571-579.
- [18] Wu J, Sun Z, Sun HS, Wu J, Weisel RD, Keating A, Li ZH, Feng ZP and Li RK. Intravenously administered bone marrow cells migrate to damaged brain tissue and improve neural function in ischemic rats. *Cell Transplant* 2008; 16: 993-1005.
- [19] Lai VK, Afzal MR, Ashraf M, Jiang S and Haider HKh. Non-hypoxic stabilization of HIF-1 α during coordinated interaction between Akt and angiopoietin-1 enhances endothelial commitment of bone marrow stem cells. *J Mol Med (Berl)* 2012; 90: 719-730.
- [20] Kwak HJ, So JN, Lee SJ, Kim I and Koh GY. Angiopoietin-1 is an apoptosis survival factor for endothelial cells. *FEBS Lett* 1999; 448: 249-253.
- [21] Gamble JR, Drew J, Trezise L, Underwood A, Parsons M, Kasminkas L, Rudge J, Yancopoulos G and Vadas MA. Angiopoietin-1 is an anti-permeability and anti-inflammatory agent in vitro and targets cell junctions. *Circ Res* 2000; 87: 603-607.
- [22] Thurston G, Rudge JS, Ioffe E, Papadopoulos N, Daly C, Vuthoori S, Daly T, Wiegand SJ and Yancopoulos GD. The anti-inflammatory actions of angiopoietin-1. *EXS* 2005; 94: 233-245.
- [23] Piao W, Wang H, Inoue M, Hasegawa M, Hamada H and Huang J. Transplantation of Sendai viral angiopoietin-1-modified mesenchymal stem cells for ischemic limb disease. *Angiogenesis* 2010; 13: 203-210.
- [24] Papapetropoulos A, Fulton D, Mahboubi K, Kalb RG, O'Connor DS, Li F, Altieri DC and Sessa WC. Angiopoietin-1 inhibits endothelial cell apoptosis via the Akt/survivin pathway. *J Biol Chem* 2000; 275: 9102-9105.
- [25] Sun L, Cui M, Wang Z, Feng X, Mao J, Chen P, Kangtao M, Chen F and Zhou C. Mesenchymal stem cells modified with angiopoietin-1 improve remodeling in a rat model of acute myocardial infarction. *Biochem Biophys Res Commun* 2007; 357: 779-784.
- [26] Toyama K, Honmou O, Harada K, Suzuki J, Houkin K, Hamada H and Kocsis JD. Therapeutic benefits of angiogenic gene-modified human mesenchymal stem cells after cerebral ischemia. *Exp Neurol* 2009; 216: 47-55.
- [27] Weir C, Morel-Kopp MC, Gill A, Tinworth K, Ladd L, Hunyor SN and Ward C. Mesenchymal stem cells: isolation, characterisation and in vivo fluorescent dye tracking. *Heart Lung Circ* 2008; 17: 395-403.
- [28] Takahashi Y, Akishima-Fukasawa Y, Kobayashi N, Sano T, Kosuge T, Nimura Y, Kanai Y and Hiraoka N. Prognostic value of tumor architecture, tumor-associated vascular characteristics, and expression of angiogenic molecules in pancreatic endocrine tumors. *Clin Cancer Res* 2007; 13: 187-196.
- [29] Kiem HP, Jerome KR, Deeks SG and McCune JM. Hematopoietic-stem-cell-based gene therapy for HIV disease. *Cell Stem Cell* 2012; 10: 137-147.
- [30] Losordo DW and Dimmeler S. Therapeutic angiogenesis and vasculogenesis for ischemic disease: part II: cell-based therapies. *Circulation* 2004; 109: 2692-2697.
- [31] Goldman S. Stem and progenitor cell-based therapy of the human central nervous system. *Nat Biotechnol* 2005; 23: 862-871.
- [32] Bao Q, Zhao Y, Niess H, Conrad C, Schwarz B, Jauch KW, Huss R, Nelson PJ and Bruns CJ. Mesenchymal stem cell-based tumor-targeted gene therapy in gastrointestinal cancer. *Stem Cells Dev* 2012; 21: 2355-2363.
- [33] Mei SH, McCarter SD, Deng Y, Parker CH, Liles WC and Stewart DJ. Prevention of LPS-induced acute lung injury in mice by mesenchymal stem cells overexpressing angiopoietin1. *PLoS Med* 2007; 4: 1525-1537.
- [34] von Dobschuetz E, Pahernik S, Hoffmann T, Kiefmann R, Heckel K, Messmer K, Mueller-Hoecker J and Dellian M. Dynamic intravital fluorescence microscopy-a novel method for the assessment of microvascular permeability in acute pancreatitis. *Microvasc Res* 2004; 67: 55-63.
- [35] Aggarwal S and Pittenger MF. Human mesenchymal stem cells modulate allogeneic immune cell responses. *Blood* 2005; 105: 1815-1822.
- [36] Ren G, Zhang L, Zhao X, Xu G, Zhang Y, Roberts AI, Zhao RC and Shi Y. Mesenchymal stem cell-mediated immunosuppression occurs via concerted action of chemokines and nitric oxide. *Cell Stem Cell* 2008; 2: 141-150.
- [37] Meng HB, Gong J, Zhou B, Hua J, Yao L and Song ZS. Therapeutic effect of human umbilical cord-derived mesenchymal stem cells in rat severe acute pancreatitis. *Int J Clin Exp Pathol* 2013; 6: 2703-2712.
- [38] Jung KH, Song SU, Yi T, Jeon MS, Hong SW, Zheng HM, Lee HS, Choi MJ, Lee DH and Hong SS. Human bone marrow-derived clonal mesenchymal stem cells inhibit inflammation and reduce acute pancreatitis in rats. *Gastroenterology* 2011; 140: 998-1008.
- [39] Edwards SS, Zavala G, Prieto CP, Elliott M, Martínez S, Egaña JT, Bono MR and Palma V. Functional analysis reveals angiogenic potential of human mesenchymal stem cells from Whar-

MSCs-ANGPT1 treatment of SAP in rats

- ton's jelly in dermal regeneration. *Angiogenesis* 2014; [Epub ahead of print].
- [40] Huang LY, Chen P, Xu LX, Zhou YF, Li WG and Yuan YZ. Fractalkine as a marker for assessment of severe acute pancreatitis. *J Dig Dis* 2012; 13: 225-231.
- [41] Uomo G, Gallucci F, Madrid E, Miraglia S, Manes G and Rabitti PG. Pancreatic functional impairment following acute necrotizing pancreatitis: long-term outcome of a non-surgically treated series. *Dig Liver Dis* 2010; 42: 149-152.